Description of ASTAVIT, a rapid assessment method of soil structural stability based on image recognition

Julien Wengler, Lionel Cottenot, Frédéric Darboux, Nicolas P. A. Saby, Marine Lacoste

HAL Id: hal-04640062
https://hal.inrae.fr/hal-04640062v1

Submitted on 9 Jul 2024

Highlights

Description of ASTAVIT, a rapid assessment method of soil structural stability based on image recognition.

Julien Wengler, Lionel Cottenot, Frédéric Darboux, Nicolas Saby, Marine Lacoste

- This work describes an alternative method for measuring aggregate stability that is less labor-intensive than traditional laboratory techniques.

- The evaluation is based on changes in the visual area of the aggregate during slaking.

- The method utilizes a 3D-printed support and well-designed LED lighting, which allows for a high throughput comparable to conventional sieving methods.

- ASTAVIT effectively distinguished between cropland and grassland, as well as different tillage practices.

Description of ASTAVIT, a rapid assessment method of soil structural stability based on image recognition.

Julien Wengler[a], Lionel Cottenot[a], Frédéric Darboux[b], Nicolas Saby[a], Marine Lacoste[a]

[a]INRAE, Info&Sols, , Orléans, 45075, France
[b]Univ. Grenoble Alpes, CNRS, INRAE, IRD, Grenoble INP*, IGE, *Institute of Engineering and Management Univ. Grenoble Alpes, Grenoble, 38000, France

Abstract

Measuring soil structure stability has always been a challenge, and various approaches have been proposed, mainly related to measuring soil aggregate stability upon wetting. This paper presents a rapid and cost-effective tool for evaluating soil structural stability named ASTAVIT, which stands for Aggregate STability Assessment using VIdeo Tests. The ASTAVIT principle involves visually monitoring the spreading of aggregates. This has already been implemented in the SLAKES smartphone application (now renamed Moulder), which simplifies the measurement of soil aggregates with minimal equipment. The aim of this work was to develop a robust, adaptable, and representative enough method that can be widely used in soil science laboratories. The protocol has been modified to use a 3D-printed plate, which source file is provided with this paper, to record the immersion of up to 96 individual aggregates in water. The increase in the projected area of the aggregates during slaking is tracked using image recognition software, ImageJ. The final stability index is determined based on this area increase. Soil structural stability can be assessed within an hour using a procedure that involves placing aggregates on a plate, filming, and analyzing. This method provides an objective evaluation of soil stability in a timely manner. The amount of soil used per test is similar to that used in Le Bissonnais tests (ISO 10930), ensuring representative results. The ASTAVIT index demonstrates expected behaviors of aggregate stability, as evidenced by its correlation with other soil characteristics and its ability to differentiate between soils that have undergone different tillage practices. An indicative classification of the ASTAVIT index into four categories of soil stability, similar to the Le Bissonnais tests, is proposed. ASTAVIT is expected to facilitate a broader implementation of structural stability studies.

Keywords: soil structure, aggregate stability, soil health monitoring, 3D-printing

1. Introduction

Soil structure can be defined as "the physical constitution of a soil material as expressed by the size, shape, and arrangement of the solid particles and associated voids, including both the primary particles to form compound particles and the compound particles themselves" [1]. This spatial organization of solid particles in soil results in a framework that can accommodate the presence and the flow of liquids and gases throughout the soil. Its conservation and improvement is a major challenge in soil

resource management to maintain environmental quality, hence active programs like the Soil Deal for Europe [2]. A good soil structure is essential for sustainable agriculture, allowing for sufficient crop productivity while enhancing water infiltration and minimizing soil erosion and degradation. Soil structure affects various physical and biogeochemical processes, including root density and growth, macropore establishment and macroporosity, water retention capacity, infiltration and surface runoff rates, soil erosion, source pollution from surface-applied chemicals, biological activity, and crop yield [3].

The stabilization of soil structure against external stresses involves various processes at different size scales, ranging from clay tactoids to micro-aggregates ($\leq 250\ \mu m$) and macro-aggregates ($\geq 250\ \mu m$) [3]. Assessing soil structure stability remains challenging due to its broad and complex nature, which cannot be summarized by a single quantity. Currently, there is no consensus on what to measure or how to measure it, resulting in a lack of reliable and easy-to-use indicators.

In practice though, the structural stability is often identified with the stability of soil aggregates and their capacity to resist breaking under the action of water or mechanical stress. Soil aggregate stability is used as an index of soil quality and it serves as a proxy to estimate the sensitivity to phenomena like soil erosion and crusting, which are difficult to measure directly.

The aggregates' structural strength can be assessed by applying energy, such as shaking, stirring, raindrop impact, or immersion in water, which generates disruptive forces within the aggregates [4, 5, 6, 7]. In particular, slaking is the tendency of soils to break down from clods into smaller aggregates under the influence of moisture changes [4], and it is of utmost importance for matters of water infiltration, erosion control and tillage practices. Our use of the term "slaking" is inspired by Emerson *et al.*[8] and designates the break-up of macro-aggregates into micro-aggregates . It is caused not only by air trapped in the aggregate [9, 10] but also by differential swelling of clay between dry and wet parts of the same aggregate during wetting [11, 12].

In this paper, we elaborate on a method of aggregate stability assessment by immersion in water, i.e. slaking experiment, without any additional mechanical energy input. The "aggregate stability tests" that we describe is used to assess the stability of macro-aggregates, by opposition with "dispersion tests" which concern the stability of the micro-aggregates. This macro-aggregates stability is believed to happen first, before the dispersion of clay occurs [3].

It should be reminded that a few other physico-chemical mechanisms are also at play when soil is wet, which are linked to capillary forces, inter-particular bonds by binding agents (clay or organic particles) and inter-particle friction. Capillary forces which need air-liquid interfaces and therefore vanish when the soil it totally wet (for example, they are essential to hold a sandcastle). They depend directly on the position and geometry of the air-water meniscii [13]. Upon wetting, the decrease in soil surface tension results in a decrease in interparticle attractive forces, which weakens the soil to, for example, raindrops. At the same time, water causes hydration, dispersion or dissolution of clay particles and other colloids, leading to structural breakdown [14]. Inter-particle friction is linked to the arrangement of the particles. Thus, capillary forces and inter-particle friction may vary as particles rearrange

during wetting/drying cycles. These wetting/drying cycles are critical for the stability of soil aggregates, but also very complex because wetting can have both negative and positive effect according to the soil nature [15].

If the structural stability of aggregates is considered an accessible indication of soil quality, we still lack a reliable, time-effective, and easy-to-implement method. For example, Emerson classified soil aggregates with a few simple physical tests, the first of which was based on the slaking behavior of the immersed aggregates [5, 16]. Field *et al.* [17] developed the ASWAT method to complete the SOILpak procedure, as alternative to end-over-end shaking procedures [18, 19] or Loveday and Pyle dispersion test [16]. Each method was either adapted to a specific type of soil or designed to mimic a particular natural phenomenon. Additionally, each indicator was not easily comparable to the others.

Recent methods for analyzing soil aggregates include updates of wet sieving protocols [4, 11, 20] or a combination of wet sieving and dry sieving with agitation [21]. Another approach involves simulating the impact of raindrops on soil aggregates using artificial rain [22], such as the Cornell Rainfall Simulator [23]. Sonic vibration can serve as a source of external mechanical stress, as demonstrated in [24, 25, 26]. To assess aggregate stability, some authors have used the evolution of water turbidity resulting from aggregate breakdown, such as Davison's turbidimeter [27] and Zhu's rapid method [28].

In the line of the wet sieving methods, Le Bissonnais *et al.* developed a normalized wet sieving method (ISO 10930) consisting of three tests: fast wetting, slow wetting, and mechanical breakdown [29, 30]. These tests provide complementary information about the soil's behavior in different conditions, e.g. light rain, heavy rain on a dry soil, raindrop impacts. Although this procedure is quite comprehensive, it is rarely measured in routine soil analysis due to the time and manpower required, as well as the lack of an available automated procedure.

The need for a fast and low-cost method of assessing aggregate stability led Fajardo *et al.* to develop a simple procedure based on the use of a smartphone, and in which individual soil aggregates are filmed during their disaggregation in water [31]. The assessed feature is the area of the aggregates as seen by the camera. The comparison between the initial area and the area during slaking results in a "slaking index", which is proportional to the area. The evolution of the total area over time was modeled using a sigmoid function, specifically the Gompertz function

$$f(x) = ae^{-be^{-cx}}, \text{where } x = \log(t), \qquad (1)$$

which allowed estimating the asymptotic area as well as the asymptotic slaking index at infinite time. This asymptotic value was the indicator of the soil stability: the higher this value, the more unstable the soil. They initially did the measurements with a Digital Single-Lens Reflex (DSLR) camera and treated the results with R software [32] [31], then a smartphone proprietary application named "SLAKES", later renamed "Moulder" in 2023, was made available [33, 34, 35]. It provided an alternate measurement, i.e. the area measurement at 10 minutes, to the estimation of the slaking index at infinite time.

Several authors have reported using the SLAKES application and evaluating its potential and limitations [36, 37, 38, 39]. Brown *et al.* identified two main limitations of SLAKES [37]. Firstly, the accuracy of the aggregate is highly dependent on lighting conditions and image contrast. Secondly, the orientation of the aggregate when

3

dropped into the petri dish is crucial for the correct interpretation of the results but is difficult to control by hand. Obour *et al.* also reported the inability in some cases to detect soil aggregates and the disaggregation process [38]. And yet, they use a selfie ring light to ensure a proper lighting. In their experiments, SLAKES failed to discriminate aggregate stabilities due to biochar amendment or crop type (maize versus okra). Rieke *et al.* applied SLAKES and three other methods to assess aggregate stability over 2,012 experimental units from 124 long-term experimental agricultural research sites in North America in the framework of soil health [39]. It was demonstrated that SLAKES is sensitive to certain management parameters, but also to climate and soil inherent properties.

Recently, the SlakeLight device, inspired by SLAKES but working in transmission, was presented by Madaras *et al.* [40]. They monitored the total amount of light intercepted by an aggregate during water slaking in small containers in a lightproof box. They were able to reliably measure 9 aggregates at a time in less than 10 minutes without any post-processing software, and were able to statistically distinguish between grassland and arable soils. Their all-in-one, easy-to-use box could indeed become a useful tool for field measurements.

The development of ASTAVIT, the Aggregate STability Assessment using Video Tests, was also initiated as a result of SLAKES' proof of concept. This method employs the same fundamental measurement of the aggregate area as the original concept, but with enhanced robustness and effectiveness. This paper presents in detail the methods and measurements employed, verifies the consistency of its results with the ISO Le Bissonnais test, discusses the choice of the stability index to be used, assesses the statistical representativity of a single ASTAVIT measurement, and proves its ability to discriminate soils undergoing contrasting management.

2. Material and methods

2.1. The measuring device

The core idea of Fajardo *et al.* [31] was kept: to monitor with a camera the evolution of the projected area of aggregates during slaking. The implementation was reviewed and modified to overcome its drawbacks: (1) the number of aggregates followed in a single measurement was dramatically increased, (2) the wetting protocol was simplified, (3) the optical detection of aggregates was improved, (4) the code was released to the community to allow further improvements.

The first two points were achieved by designing a 3D printed immersion device on which up to 96 aggregates with a size of 3-5 mm are placed in a rectangular array and then immersed while being filmed. Thus, in the ASTAVIT protocol, an amount of about 5 g of soil is used, that is the amount used in a single Le Bissonnais test [29, 30].

The figure 1A shows the model of this immersion device which was 3D-printed in PETG (polyethylene terephthalate glycol) on an Ultimaker 2+ printer. The device comprises two distinct parts. The first part is a rectangular plate that has an array of 96 boxes designed to hold the aggregates. At the intersections of the grid that delimits these boxes, there are 4 mm diameter holes that allow water to flow through and rise from under the plate. The second part is a tray that accommodates the plate and has a reservoir positioned on its side (located at the bottom-left of fig 1A). The plate is intended to be detached from the tray to simplify the process of cleaning soil residues that
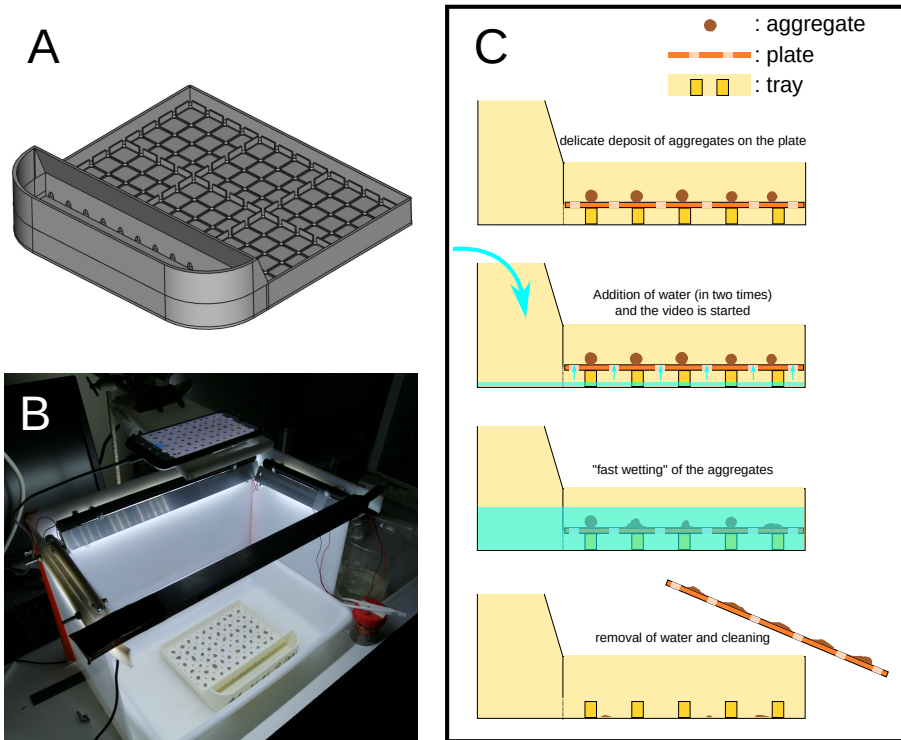
Figure 1: Design of the immersion device and procedure. A: 3D View of the 3D-printed immersion device. The plate can hold 96 individual aggregates. B: View of the complete experimental setup with the smartphone and LED lighting. C: Schematic side view illustrating the use of the tray. Water is poured into the reservoir on the left and allowed to flow under the plate containing the aggregates. As the water continues to fill, it flows out through holes in the plate and the aggregates are submerged. At the end, the plate is removed for cleaning.

may pass through the holes. The size of these elements, and therefore the number of aggregates it can accommodate, was only limited to the maximum printing area of the 3D-printer and could be enlarged.

The protocol is as follows (Fig. 1C): place the plate on the tray and carefully position the aggregates, one in each box to prevent mixing. Pour around 200 mL of deionised water in the tray to fill its lower part while staying below the plate. Start the recording by the smartphone camera, and pour around 400 mL more water into the tray to completely submerge the aggregates. This method ensures that the aggregates remain stationary during wetting, preventing them from rolling over. As a result, the evolution of their surface area is solely due to slaking. The smartphone is placed horizontally above the immersion

device so as to ensure that all aggregates are visible within the picture frame. Since adequate lighting is crucial to the measurement quality, we utilized an LED strip that formed a rectangular shape above the immersion device (similarly to what is done with photography boxes), positioned at a height roughly equal to that of the smartphone (Fig. 1B). The LED rectangle should be sufficiently large to prevent direct reflection of light on the water surface toward the camera. Video recording was set to 30 minutes at a rate of 1 frame per second using the OpenCamera application (setting speed × 30 to get 1 frame per second) [41]. Any other video application may be used, as long as the recording rate is editable. The plate geometry was designed to have the same aspect ratio as the picture to prevent the need for manually cropping extra-

neous features outside of the plate. In a preliminary test, two video resolutions were used: 1920×1080 for a 16:9-shaped 60-aggregate plate, and 720×480 for a 4:3-shaped 96-aggregate plate. Results showed that resolution is inconsequential in this context. The video files were then imported and treated with the Fiji variant of ImageJ [42] using the ffmpeg plugin and a dedicated code (see electronic supplementary material). The code monitors the cumulative aggregate area of the entire frame. It provides an average value that is representative of the overall behavior of the whole soil sample.

The video treatment with imageJ is illustrated in figure 2 and the script is given in appendix Appendix A. The images have a light background as the plate and tray were printed with white material, while the aggregates are somewhat darker (Fig. 2-A). To separate aggregates from background, the imageJ script performs the following operations on each individual picture. The pictures are converted to gray scale and inverted so that the lower values correspond to the background (initially white or light color) (Fig. 2-B). In order to highlight the aggregates, the value of the background is subtracted. This value is approximated by taking the median brightness value of the whole frame, since more than 50% of the total frame area is constituted by the rather homogeneous low-valued background, the rest being the higher-valued aggregates (Fig. 2-C). This allows for the Fiji automatic threshold to accurately separate the soil aggregates or particles from the plate (Fig. 2-D). At that point, an additional particle analysis was initially performed to address the issue of holes in the plate being detected as soil particles due to their slightly darker appearance compared to the plate background. To eliminate these unwanted features,

a minimum particle area was manually set. This analysis is shown on Fig. 2-E even though it was not strictly necessary: the dark color of the soil provided a strong enough contrast. In some cases, experience has shown that using a lightly colored plate instead of a completely white plate and a white tray can reduce the contrast of the holes and the likelihood of detection errors. For the initial frame with the dry aggregates, particle analysis is still necessary because the contrast of the holes appear stronger than with water. It is crucial to obtain an accurate measurement of the initial aggregate area for subsequent calculations. Therefore, only the n greatest detected particles are kept, corresponding to the n expected aggregates ($n = 60, 96$ or possibly less if the plate is not full, this figure is manually inputted in the script file). Eventually, a measurement of the total area yields the aggregates total projected surface area.

The measured quantities were the initial area of the ensemble of soil aggregates S_0, and their area every second, allowing to obtain the curve of the aggregates area in function of time $S(t)$. The Gompertz function (equation 1) was used to fit the points, with S_0 as the initial area, according to equation (2).

$$S(t) = S_0(1 + ae^{-be^{-c\log(t)}}) \qquad (2)$$

The slaking index $SI(t)$ as introduced by Fajardo *et al.* [31] was defined by the ratio $\frac{S(t)-S_0}{S_0}$. Its value at infinite time SI_∞ is obtained from the curve fitting: the coefficient a is directly equal to SI_∞.

In addition to this indicator, we attempted to use some variants. Firstly, it is possible to use the decimal logarithm of the ratio of the final value, SI_∞, to the initial value, S_0, that is, $\varsigma_\infty = \log\left(\frac{S_\infty}{S_0}\right) = \log(1 + SI_\infty)$. This index may be considered as a potential substitute for the original index.
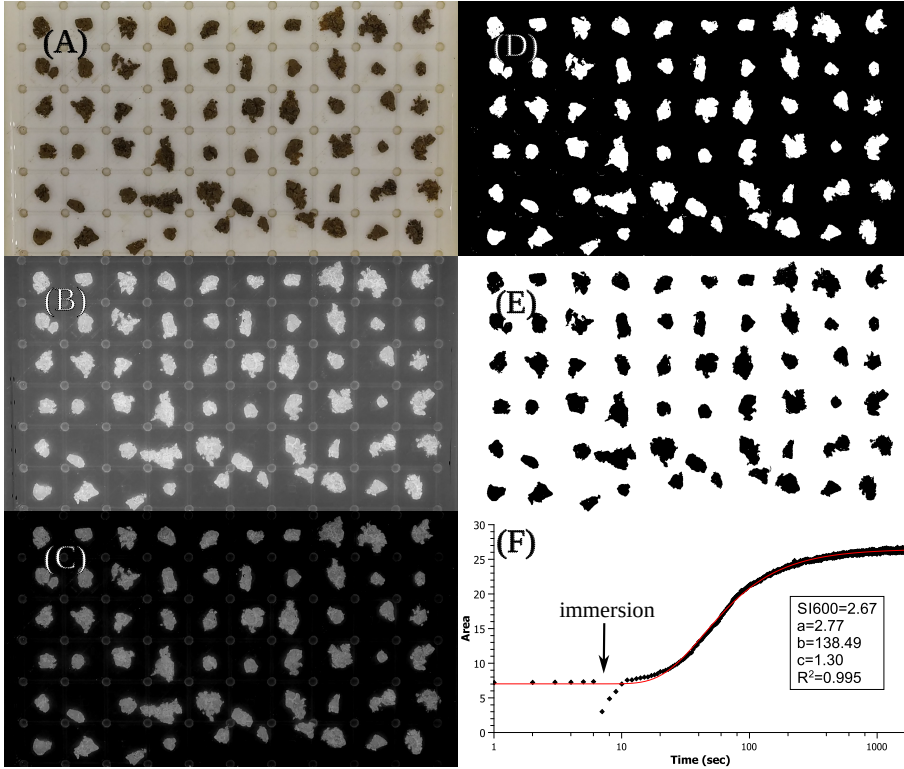
6

Figure 2: Illustration of the image processing algorithm and its output. (A) Raw image. (B) Grayscale and inverted. (C) Median value subtracted. (D) Image after automatic thresholding. (E) Particle analysis. (F) Output curve of the aggregate area versus time and the different indexes calculated. Note the moment when the aggregates are immersed: at first, during the flow of water, it is difficult to detect correctly the aggregates. Hence, the importance of the separate initial-area calculation.

The rationale behind this choice will be explained in more detail in the subsequent sections of the paper. Secondly, it was observed that both SI_∞ and ς_∞ solely consider the value at the final state of the aggregates, without accounting for the slaking dynamics. Consequently, we put forth the proposition of employing the quantity $\tau = \left(\dfrac{b}{\ln 2} \right)^{1/c}$, defined as the time required for the Gompertz function to reach half of its final value, or even the quantity SI_∞/τ, which is approximately equal to the rate at which slaking occurs.

2.2. The soil samples and soil data

We used data from the French Soil Quality Measurement Network (RMQS, "Réseau de Mesure de la Qualité des Sols"). This extensive soil database comprises soil data from points all over France at the nodes of a 16×16 km² grid [43].

Table 1: Range of variation of physico-chemical properties of the 145 RMQS sites used for the stability assessments.

	Min value	Max value
Clay (%)	8.2	56.3
Silt (%)	10.4	79.8
Sand (%)	1.9	81.0
Organic matter (%)	0.51	9.37
pH (water)	4.3	8.4
Ca^{2+} (mg/kg)	1	41
CEC (cmol(+)/kg)	0.800	42.5

Aggregate stability measurements were carried out on 145 of these sites (89 cropland, 44 grassland, 4 fallow,

3 cultivated grassland, 2 vineyard, 1 legumes, 2 woodland) which are representative of the variability of French soils (see table 1). Soil stability was assessed using three protocols. First, the Le Bissonnais method [29] provided the current reference measurements for 134 of these sites, of which we looked specifically at the rapid wetting test as it is the closest to the operating mode of the two other methods. Then, additional measurements were carried out with the SLAKES application [34, 44] using groups of 3 aggregates with repetitions up to 12 to 70 aggregates. The experiment's time constraints strongly limited the number of repetitions, resulting in priority being given to certain sites over others: 90 sites were measured using this method. Lastly, structural stability was measured using the ASTAVIT method on the 131 sites for which aggregates were still available.

To test the results of ASTAVIT on soils differing only by their tillage practices, we used two couples of samples. The first couple of samples were collected from an experimental plot of the "Institut Technique des Céréales and Fourrages" at Boigneville, France. This clay loam was tilled either by conventional tillage (CT) or by direct drilling (DD). The plots with these treatments were established in 1970. The sampling was done in the 0-15 cm depth. The second couple of samples came from the EFELE platform which aimed at studying the impact of residual organic products [45], and more specifically from fields of the experimental plot TS-MO on which tillage practices coupled with organic matter fertilization were investigated. Since 2012, twelve plots have been cultivated using a wheat-maize rotation and white mustard intermediate crops, with varying tillage and fertilization methods: plowing (P) versus simplified tillage (ST), and mineral (MIN) versus cattle manure (CM) fertilization. In 2017, soil samples were collected from the 0-15 cm layer. Here, we consider the mineral fertilization condition, and compared the P and the ST treatments.

The Boigneville soils underwent four tests using our method, resulting in 276 individual aggregates (three experiments with 60 aggregates and one experiment with 96 aggregates). Regarding EFELE samples, there were two plots with simplified tillage and four plots with plowing. Two measurements were performed for each of them, one with 60 aggregates and another with 96 aggregates, resulting in a total of 936 aggregates.

2.3. Statistical assessments

Additionally, we sought to ascertain the degree to which a single ASTAVIT measurement would be representative, or the number of repetitions that would be necessary to obtain a reliable result for a given soil. To quantify this, we considered both intra-measure and inter-measure variabilities. The intra-measure variability characterizes the variability of individual aggregates in a single measurement. In contrast, inter-measure variability explores the variability between the global results of multiple measurements on the same soil.

The intra-measure analysis was conducted on five soils from RMQS that were selected because they exhibited contrasted stabilities and compositions (table 4). Videos of 60-aggregate immersion experiments (with the preliminary device capable of holding only 60 aggregates) were recorded. Instead of analyzing the entire frames, they were cropped to allow the analysis script to be run on subsets of three aggregates, mimicking the SLAKES application, but carrying out 20 measurements simultaneously. For each soil, we calculated the mean and standard de-

viation of these 20 measurements, and then assessed the minimal number of 3-aggregates samples needed to reach an accuracy of ±10% of the mean with a confidence level of 95% using the formula

$$n = \sqrt{\frac{Z\sigma}{E}} \qquad (3)$$

where Z is the score corresponding to the desired confidence level (here 1.96, since we selected a 95% confidence level), σ is the evaluated standard deviation of the samples, and E is the desired margin of error, expressed as an absolute value, here 10% of the mean. We then multiplied the result by 3 to get the minimal number of aggregates to be measured.

The inter-measurement variability was carried out by comparing multiple immersion measurements on the same soil from the Boigneville site (see previous section). Four repetitions of the 60-aggregate immersion experiments were conducted to obtain data on aggregates from both tillage practices.

3. Results

3.1. Comparison with the SLAKES application measures

For all the RMQS samples which have undergone both types of measures, we plotted the ASTAVIT SI_∞ index against the SLAKES application index (fig. 3). We found a good linearity, with a Pearson coefficient of determination is $R^2 = 0.557$. However, we can notice a systematic bias from the 1:1 line, which means that either ASTAVIT underestimates the slaking index, or SLAKES overestimates it.

3.2. Comparison with Le Bissonnais method

One reference method for measuring aggregate stability is the normalized Le Bissonnais tests. It was important
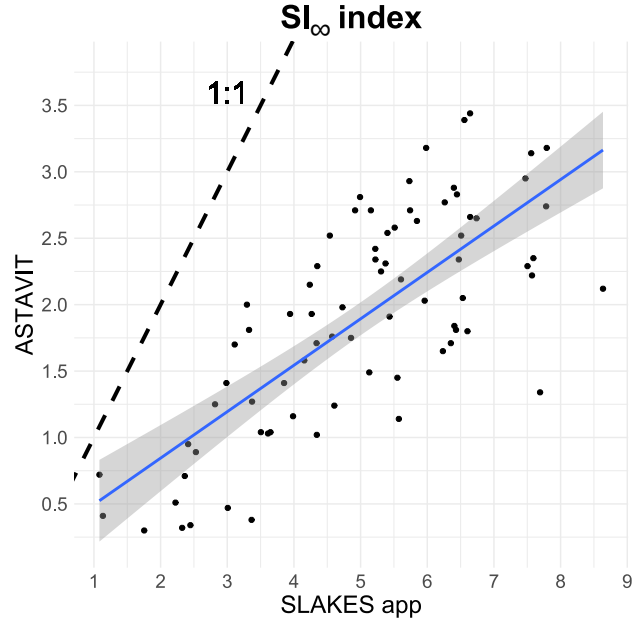

Figure 3: Comparison of the soil stability measurements obtained on RMQS soil samples with the SLAKES application and with the ASTAVIT protocol.

to determine if the ASTAVIT results were consistent with those obtained using that method. Among the three tests involved in Le Bissonnais protocol – rapid wetting, slow wetting, and stirring after pre-wetting – only the rapid wetting test and its subsequent mean weighted diameter (MWD) index were considered, as the experimental conditions were deemed to be the closest to those used in the ASTAVIT.

The figure 4A shows the correlation between the measurements made on the RMQS samples either with the Le Bissonnais rapid wetting test or with ASTAVIT. The resulting graph has a negative slope because a more stable soil means a low ASTAVIT index but a high MWD. The graph suggests a non-linear behavior (see LOESS fitting) and a saturation for the least and most stable aggregates.

The MWD does not go below about 0.250 mm, which is the generally accepted boundary between micro-aggregates and macro-aggregates. This is consistent with the fact that

9

disaggregation by slaking only affects macro-aggregates, while micro-aggregates integrity is only compromised by clay dispersion. The ASTAVIT SI_∞ index, on the other hand, seems to tend to a non-zero value for the most stable aggregates. This value corresponds to a few tens of percent increase in size and corresponds to clay swelling without macro-aggregate disruption.

The general shape of the plot suggests a power-law relationship. A plot of MWD against the square root of SI_∞ (plot not shown) actually showed better linearity, consistent with the fact that MWD is a length measure while SI_∞ is an area measure. To be more general, we decided to use a logarithmic scale instead of $SI(t)$ and introduced a new notation, i.e. $\varsigma_\infty = \log\left(\frac{S_\infty}{S0}\right) = \log(1 + SI_\infty)$. Such a logarithmic transformation was already done in earlier works [39, 38]. The figure 4B confirms the better linear fitting and an increase of R^2, from 0.6406 with SI_∞ to 0.6857 with ς_∞.

Notice also the enhancement with regards to the coefficient of determination R^2 of the SLAKES data against Le Bissonnais rapid wetting MWD which was only 0.532. This indicates better overall coherence of ASTAVIT results with Le Bissonnais results and is likely due to the reduction of experimental uncertainties in the ASTAVIT method compared to the earlier SLAKES method.

In his method, Le Bissonnais *et al.* [29] introduced qualitative limits to relate the absolute values of the MWD values to the stability of a soil. They were set at 0.4 mm, 0.8 mm, 1.3 mm, and 2 mm, delimiting 5 categories (Table 2) shown in Figure 4B as green vertical dotted lines. Likewise, we have visually estimated a similar partitioning with respect to the value of ς_∞ based on the distribution of the data points and shown on Figure 4B as green

horizontal dotted lines. Thus, soils may be classified into four categories based on their stability, ranging from very unstable to very stable, with limits at $\varsigma_\infty = 0.25, 0.4$, and 0.55 (see table 2). These somewhat arbitrary limits are only intended to give a qualitative indication of the stability of a soil: the primary role of the ASTAVIT index is to compare samples, not to assign an absolute value to a soil.

3.3. Choosing the best indicator

In addition to the ς_∞ index which relies solely on the final state of the aggregate slaking experiment, more indices might be used to characterize the dynamics of the disaggregation, such as τ and $Asym/\tau$ (see section 2.1). In order to assess their physical relevance, we tested the correlation of the three indicators ς_∞, τ and $Asym/\tau$ with soil properties which are known to affect soil stability and soil usage.

Among the RMQS samples, we kept only those which were either grassland or cropland, which made 125 samples. For each indicator as outcome variable, we performed a multiple linear regression in R with distinct predictor variables: clay content, silt content, organic matter content (OM), Na^+ concentration, Ca^{2+} concentration, pH in water, cationic exchange capacity (CEC), soil usage (here cropland or grassland). The best fits with the minimum relevant variables are listed in Table 3. Only variables yielding a p-value< 0.05 were kept. We clearly see that only ς_∞ exhibits a signification agreement with the soil properties. This lead us to reject the use of τ and $Asym/\tau$ and confirm the use of ς_∞.

3.4. Consistency of ASTAVIT with current knowledge

As a further illustration, a mapping of the correlation coefficients between ς_∞ and its relevant soil variables is

10

Table 2: Absolute stability partitioning according to the value of the Le Bissonnais MWD (in millimeters) on the one hand and of the ASTAVIT's ς_∞ value on the other hand.

MWD < 0.4	0.4 < MWD < 0.8	0.8 < MWD < 1.3	1.3 < MWD < 2	MWD > 2
very unstable	unstable	medium	stable	very stable

ς_∞ < 0.25	0.25 < ς_∞ < 0.4	0.4 < ς_∞ < 0.55	ς_∞ > 0.55
very stable	intermediate	unstable	very unstable

Table 3: Optimal multiple linear regression for ς_∞, τ and $Asym/\tau$ in function of the soil variables – clay content, silt content, organic matter content, Ca^{2+}, Na^+, cationic exchange capacity (CEC) and soil usage. Only variables yielding a p-value< 0.05 were kept. For $Asym/\tau$, no variable was statistically relevant, and the R^2 value is the one found when all variables are included in the regression.

ς_∞ (stability ↗ if ↘)				τ (stability ↗ if ↘)				$Asym/\tau$ (stability ↗ if ↘)			
Parameter	**Estimate**	**p-value**	**Signif.**	**Parameter**	**Estimate**	**p-value**	**Signif.**	**Parameter**	**Estimate**	**p-value**	**Signif.**
OM (%)	-0.0470696	5.80e-08	***	OM (%)	19.1031	6.02e-09	***	-	-	-	-
CEC	0.0284004	9.62e-05	***	clay (%)	-1.4482	0.001211	**				
Ca^{2+}	-0.0250860	0.000249	***								
soil.use	-0.0697782	0.008418	**								
silt (%)	0.0014406	0.003794	**								
Global R^2	**0.6281**			**Global R^2**	**0.2558**			**Global R^2**	**0.0417**		

presented in Figure 5. It is evident that the behavior of the soil, and more specifically its stability, differs quantitatively between grassland and cropland. In both cases, the variables the most correlated to ς_∞ is the organic matter content of the soil. However, the values of the regression coefficients differ. Additionally, grassland data exhibit greater heterogeneity, which makes the identification of a statistically significant correlation formula more challenging.

In summary, the observed behaviour is consistent with common knowledge in soil science and can be described as follows: an increase in stability is evident with an increase in clay content, organic matter content, calcium content, CEC, and with a decrease in silt content.

Concerning land usage, results of ASTAVIT measurements for grassland and cropland soils are indeed statistically different (Student Test, p = 7.668 10^{-14}, see figure 6), as expected [46].

Another property we want to test is the ability of AS-TAVIT to discriminate between soils that have been subjected to different management practices, such as tillage. For this we used the soil samples from the Boigneville and EFELE sites. The results are shown in Figure 7 where the visual separation of the box plots and the statistical tests allow to conclude that ς_∞ is able to discriminate between the studied tillage practices.

3.5. Evaluation of the statistical uncertainties

Firstly, the final line of Table 1 presents the intra-measurement variability measurements on the five chosen RMQS soil samples. It can be observed that, depending on the sample under consideration, either approximately 20 or approximately 80 aggregates must be probed in order to obtain a result that is within 10% of the mean value. This bipolar distribution suggests the existence of two regimes: one for the extremes (either very unstable

Table 4: Estimation, for 5 soils from RMQS of contrasted stability, of the number of aggregates needed in a measurement for the result to have 95% chances of being in the interval ±10% from the mean value of measured on the whole aggregate plate.

RMQS identifier	0012	0006	0816	1088	1078
Clay (%)	21.5	24.7	34.8	25.5	49.2
Silt (%)	50.8	25.3	55.0	50.2	26.1
Sand (%)	27.7	50.0	10.2	24.3	24.7
OM (%)	5.10	2.22	4.27	1.90	2.46
pH (water)	7.5	8.2	5.9	7.1	8.0
Ca^{2+}	18.31	16.25	13.8	11.91	33.34
CEC (cmol(+)/kg)	20.2	17.4	16.4	13.8	38.5
ς_∞	0.290	0.441	0.487	0.524	0.617
Number of aggregates needed	19	77	79	18	20

or very stable) with a low variability and a second for soils of intermediate stability with a high variability. In the first case, all aggregates tend to be either totally stable or totally disaggregated, whereas for intermediate stabilities, we have a comparable amount of rather stable or rather unstable aggregates, and randomness of the sampling yields a greater impact on the resulting stability index. In other words, it can be said that there is greater entropy in soils with intermediate stability, and less entropy in soils with extreme stability. This is analogous to the textbook case of the two-level system.

In any case, these results allow us to conclude that a single immersion experiment with 96 aggregates is sufficient to satisfy the established criterion and to maintain the relative error bars of ς_∞ at approximately 10%.

Secondly, the inter-measurement variability was assessed by determining the $\pm 1.96\sigma$ interval of the ς_∞ distribution obtained by repeating the 60-aggregate ASTAVIT protocol on samples from Boigneville sites. This interval corresponded to ±5% and ±15% of the mean value for conventional tillage and direct-drilled plots, respec-

tively. This is consistent with the two previously described regimes, as the ±5% interval corresponds to the highly unstable soil (low variability), while the ±15% interval is indicative of moderately stable soil (high variability). In the most unfavorable scenario, a single 60-aggregate ASTAVIT measurement has a 95% probability of being less than 15% apart from the mean value of a multitude of measures. The degree of accuracy would be significantly enhanced with the 96-aggregate ASTAVIT measurement system.

When these results are considered collectively, it can be concluded that a single 96-aggregate ASTAVIT test is sufficient if the desired accuracy is within a ±10% range (with a 95% certainty).

4. Discussion

Although the original Slakes experiment by Fajardo *et al.* [31] was conducted in a laboratory setting, it has subsequently evolved to become available to various agricultural practitioners and stakeholders. This has been achieved through the development of a mobile application, which

has been evaluated by Flynn *et al.* [47, 34]. Other projects, such as the SlakeLight device [40], have a similar goal and may be well suited for field use because they are completely self-contained and easy to use. But they are proprietary and not easily replicable. In contrast, ASTAVIT may be regarded as a derivative of the SLAKE principle, designed for use in soil laboratories. The greater need for additional material, such as proper lighting for 3D printing, is offset by the greater measurement efficiency of the ASTAVIT, which can measure ten times as many aggregates as SlakeLight.

A prolonged period of experimentation with the SLAKES application within our laboratory revealed that it was unable to fulfill the requisite accuracy and throughput standards for soil analysis and research. This was attributed to the limited number of aggregates that could be utilized simultaneously, as well as certain inherent limitations of the application, including a suboptimal segmentation algorithm and an inability to zoom in or adjust the focus. For instance, a systematic error was introduced by an underestimation of the aggregate area, which is proportionately more significant for smaller aggregates, i.e., prior to slaking. This resulted in the observed systematic bias depicted in Figure 3.

In contrast, ASTAVIT offers substantial time and ease-of-use advantages. The method allows the operator to measure 96 aggregates per soil sample in less time and in a single experiment. This reduces the risk of handling errors and improves the reproducibility of the results. Furthermore, the simple design of the LED illumination and the optimisation image treatment ImageJ script permitted the accurate detection of aggregates, regardless of room lighting conditions or soil type. The initial surface area of the aggregates is reliably evaluated before wetting, as this process strongly influences the final stability index. This is because the aggregates hardly move or roll over when they are immersed. In the script utilized for image treatment in ASTAVIT, the decision was made not to treat aggregates as separate entities but rather as a collective unit, with the focus being on the detection of the cumulative surface area. This approach allowed for the direct determination of the average slaking index of the aggregates.

The ASTAVIT index, ς_∞, exhibited a robust qualitative correlation with the reference Le Bissonnais rapid wetting test (Figure 4), despite the dispersion of the data points. The 12-year temporal gap between the Le Bissonnais stability measurements (2010–2012) and the ASTAVIT experiments (2023) is a contributing factor to this dispersion. During this period, the dried lumps of soil were indeed kept in a box and subjected to aging. One limitation of the ASTAVIT method is illustrated by the saturation of ς_∞ at a non-zero value for very stable aggregates due to clay swelling. Hence, for $\varsigma_\infty < 0.2$, the influence of soil texture via clay swelling is the dominant factor, and must be taken into account when comparing experiments conducted on different soils.

The reliability of ASTAVIT measurements has been validated through the demonstration of high reproducibility within a given batch of soil aggregates. One ASTAVIT experiment involves 96 aggregates, which is approximately equivalent to the 5 g sample used for a single Le Bissonnais test. In terms of representativeness, the ASTAVIT method is at least as effective as the Le Bissonnais method for a single measurement. The capacity of the ASTAVIT technique to yield a relevant result with a single measure,

with an error margin of only 10%, represents a significant advantage.

In terms of experimental duration, there is no significant gain from Le Bissonnais to ASTAVIT if we consider only the rapid wetting test. In the former, half an hour is generally sufficient to perform three replicates, while in the same time, three ASTAVIT experiments can also be performed in parallel. The original duration of an ASTAVIT experiment was set at 30 minutes to ensure reliable preliminary results. However, this duration can be reduced to 10 minutes for routine use of the method. The parallelization of ASTAVIT experiments can also be a time-saving measure, provided that the laboratory has sufficient immersion devices, light boxes, and cameras.

Other advantages of ASTAVIT over Le Bissonnais are as follows. 1- Ethanol is not needed for any wet sieving, reducing safety concerns. 2- The results can be obtained rapidly through computer analysis, without the need for a 48-hour drying period before the final dry sieving. 3- There is no need for an oven at all. 4- There are no steps of aggregate transfer or manual sieving that could introduce operator-related biases.

The ASTAVIT test, as described in this paper, corresponds to the Le Bissonnais rapid wetting test. While it may appear to be a more reductive test, a minor adaptation of the protocol can result in the ASTAVIT test mimicking the behavior of the slow wetting test. For example, one might consider placing a sheet of filter paper on the plate prior to the addition of the aggregates. Subsequently, an appropriate quantity of water would be added to wet the filter paper without submerging the aggregates, allowing the aggregates to wet by capillarity for a period of 30 minutes before being immersed and monitored in accordance with the standard ASTAVIT methodology.

In fact, the protocol can be modified in numerous ways to accommodate a wide range of needs, as exemplified by the following.

A- ASTAVIT can be utilized in conjunction with backlighting, either through the use of a translucent immersion device analogous to the improvement proposed by Madaras to the SLAKES protocol [40], or through the deployment of a UV-illuminated fluorescent plate, which has been successfully validated in our laboratory. In both instances, the presence of aggregates is indicated by their detection as shadows cast by the light source, and the influence of soil color on the outcome is no longer a factor.

B- One can simplify the process by considering only the value of the slaking index at a given time, rather than employing curve fitting. This approach was proposed by Flynn and colleagues in their 2020 evaluation [34] where the value of $SI(t)$ at 10 minutes, $SI_{600} = \frac{S(600) - S_0}{S_0}$ was utilized as a reliable approximation of SI_∞. The number of required images would be reduced to two, although the results may be subject to alteration in the case of soils with a longer typical slaking time.

C- Stirring may be introduced to test the influence of mechanical stress on slaking, possibly after saturation with ethanol as in the third Le Bissonnais test.

D- The device can lastly be adapted for studies of the disaggregation mechanisms, e.g. by changing the electrolyte concentration and the sodium adsorption ratio of the solution used, as suggested by Amezketa et al. [3], or by using tensio-active compounds like in the work of Zaher et al. [10].

We would like to conclude this discussion with insights into the applicability of the ASTAVIT stability in-

dex and its positioning among competing methods. It is important to note that the categorization of ς_∞ values proposed in this paper must be considered indicative, in a similar fashion to the categorization proposed by Le Bissonnais. Given the variability and multifactorial nature of soil aggregate stability, the interpretation of its absolute value is open to debate. The most prudent use of ς_∞ is to compare samples that have already been adequately described and whose differences and common points are already known.

Some authors have cautioned against the use of a single indicator for crusting sensitivity assessment, citing the need for a multi-indicator approach [48]. The selection of an indicator is contingent upon the specific aspect being evaluated, the environmental conditions under which the assessment is conducted, the sampling date and methodology, and other pertinent variables. There is no universal index for assessing structural stability, particularly when studying the potential for crusting or erosion. The objective is to compare different soils in space or time with respect to a given property or management practice [29]. In this regard, the ASTAVIT test is comparable to the Le Bissonnais test and should be regarded as an additional method for assessing aggregate stability.

Given the lack of a single method of aggregate stability measurement that stands out as clearly superior [39], the choice for this or another method will be determined by the budgets and equipment available or the increased sensitivity to a specific management practice. It is important to note that different methods are not mutually consistent and are not interchangeable [39].

The objective of ASTAVIT is not to establish a consistent correlation between aggregate stability and soil erodi-

bility or crusting potential. Furthermore, it is not intended to supersede the current standard method. Instead, it serves as a valuable instrument for the conduct of investigations into soil stability. It is recommended that the method be employed after a clear objective has been defined, such as a spatial comparison between two plots with different agricultural practices or a temporal tracking of the properties of a given soil.

5. Conclusion

We presented the ASTAVIT method, which is a rapid, universal, adaptable, and straightforward tool for assessing soil aggregate stability. The method is relatively simple to operate, requiring only a few basic elements. These include a 3D-printed immersion device (plate + tray), a smartphone, and a computer with the ImageJ open-source software. ASTAVIT is consistent with the Le Bissonnais rapid wetting test. We have identified the ς_∞ as a relevant stability index that correlates positively with known soil properties, including organic matter content, texture, and land usage. The capacity of ASTAVIT to differentiate between tillage practices (tillage vs. no-till) was demonstrated in two experimental plots.

A single 96-aggregate experiment provides a rapid and accurate assessment, with a standard deviation of the order of 10% for a given batch of aggregates (same soil, same field sampling, same aggregate fabrication). Furthermore, it is anticipated that this test will be applicable to a diverse range of soil types and behaviours with a single setup, due to its capacity to probe the full slaking dynamics.

The objective of ASTAVIT is not to supplant other reference stability measurements; rather, it is intended to

serve as a convenient tool to facilitate the conduct of soil stability surveys, such as inter-crops comparisons or temporal follow-ups. It is crucial to note that the findings of the study are only meaningful when considered in the context of the study's objective. As with the other methods, particular attention should be paid to the sampling and fabrication of aggregates, as these factors are highly dependent on the operator.

By measuring the stability of a representative quantity of 96 aggregates in 30 minutes, the ASTAVIT method is a rapid and statistically relevant method for soil stability tests in laboratories. Further optimization for routine work may be achieved by reducing the test duration to 10 minutes and by parallelizing the experiments. It would be beneficial to improve the hydrophilicity of the plate in order to facilitate the wetting of the aggregate by rising water, thereby reducing experimental variability. In the future, the entire protocol, including image and data analysis, could theoretically be adapted to a smartphone application, as has been done with SLAKES/Moulder.

Finally, it is believed that a variation of the ASTAVIT protocol, in which the aggregates first undergo slow wetting, would be beneficial for a more complete study of soil aggregate behavior and its underlying disaggregation mechanisms.

Appendix A. Supplementary material

The ASTAVIT_sample_raw_video.mp4 file provides an example of raw ASTAVIT video footage.

Both the STL files of the 96-well immersion device and the ImageJ image recognition script may be shared via a simple e-mail request to the corresponding author.

References

[1] R. Brewer, J. R. Sleeman, Soil Structure and Fabric, Journal of Soil Science 11 (1960) 172–185. doi:10.1111/j.1365-2389.1960.tb02213.x.

[2] E. Commission, EU Mission: A Soil Deal for Europe, 2024. URL: https://research-and-innovation.ec.europa.eu/funding/fund

[3] E. Amézketa, Soil Aggregate Stability: A Review, Journal of Sustainable Agriculture 14 (1999) 83–151. doi:10.1300/J064v14n02_08.

[4] R. E. Yoder, A Direct Method of Aggregate Analysis of Soils and a Study of the Physical Nature of Erosion Losses1, Agronomy Journal 28 (1936) 337–351. doi:10.2134/agronj1936.00021962002800050001x.

[5] W. Emerson, A classification of soil aggregates based on their coherence in water, Soil Research 5 (1967) 47. doi:10.1071/SR9670047.

[6] E. A. Matkin, P. Smart, A comparison of tests of soil structural stability, Journal of Soil Science 38 (1987) 123–135. doi:10.1111/j.1365-2389.1987.tb02130.x.

[7] R. A. Young, A Method of Measuring Aggregate Stability Under Waterdrop Impact, Transactions of the ASAE 27 (1984) 1351–1354. doi:10.13031/2013.32970.

[8] W. W. Emerson, D. J. Greenland, Soil Aggregates — Formation and Stability, Soil Colloids and Their Associations in Aggregates (1990) 485–511. doi:10.1007/978-1-4899-2611-1_18.

[9] H. Zaher, J. Caron, B. Ouaki, Modeling Aggregate Internal Pressure Evolution following Immersion to Quantify Mechanisms of Structural Stability, Soil Science Society of America Journal 69 (2005) 1. doi:10.2136/sssaj2005.0001.

[10] H. Zaher, J. Caron, Aggregate slaking during rapid wetting: Hydrophobicity and pore occlusion, Canadian Journal of Soil Science 88 (2008) 85–97. doi:10.4141/CJSS07021.

[11] W. D. Kemper, R. C. Rosenau, Aggregate Stability and Size Distribution, in: Methods of Soil Analysis, John Wiley & Sons, Ltd, 1986, pp. 425–442. doi:10.2136/sssabookser5.1.2ed.c17.

[12] R. S. Murray, J. P. Quirk, Intrinsic Failure and Cracking of Clay, Soil Science Society of America Journal 54 (1990) 1179–1184. doi:10.2136/sssaj1990.03615995005400040044x.

[13] M. Scheel, R. Seemann, M. Brinkmann, M. Di Michiel, A. Sheppard, B. Breidenbach, S. Herminghaus, Morphological clues to

16

wet granular pile stability, Nature Materials 7 (2008) 189–193. doi:10.1038/nmat2117.

[14] B. D. Kay, A. R. Dexter, Influence of aggregate diameter, surface area and antecedent water content on the dispersibility of clay, Canadian Journal of Soil Science 70 (1990) 655–671. doi:10.4141/cjss90-068.

[15] K. Denef, J. Six, H. Bossuyt, S. D. Frey, E. T. Elliott, R. Merckx, K. Paustian, Influence of dry–wet cycles on the interrelationship between aggregate, particulate organic matter, and microbial community dynamics, Soil Biology and Biochemistry 33 (2001) 1599–1611. doi:10.1016/S0038-0717(01)00076-1.

[16] J. Loveday, J. C. Pyle, The Emerson Dispersion Test and Its Relationship to Hydraulic Conductivity, Melbourne, Vic., CSIRO Division of Soils, 1973. doi:10.25919/jvpw-ya58.

[17] D. Field, D. McKenzie, A. Koppi, Development of an improved Vertisol stability test for SOILpak, Australian Journal of Soil Research 35 (1997) 843–852. doi:10.1071/S96118.

[18] H. E. Middleton, Properties of Soils Which Influence Soil Erosion, U.S. Department of Agriculture, 1930.

[19] J. Quirk, The measurement of stability of soil micro-aggregates in water, Australian Journal of Agricultural Research 1 (1950) 276–284. doi:10.1071/AR9500276.

[20] E. Kandeler, Aggregate stability, in: Methods in Soil Biology, schiner et al. ed., Springer-Verlag, Berlin, 1996, pp. 390–395.

[21] A. J. Franzluebbers, S. F. Wright, J. A. Stuedemann, Soil Aggregation and Glomalin under Pastures in the Southern Piedmont USA, Soil Science Society of America Journal 64 (2000) 1018–1026. doi:10.2136/sssaj2000.6431018x.

[22] AJ. Low, Measurement of stability of moist soil aggregates to falling waterdrops according to Low, West-European methods for soil structure determination (1967) 51–78.

[23] B. N. Moebius-Clune, D. J. Moebius-Clune, B. K. Gugino, O. J. Idowu, R. R. Schindelbeck, A. J. Ristow, H. M. van Es, J. E. Thies, H. A. Shayler, Comprehensive Assessment of Soil Health, 3rd edition ed., Cornell University, 2016. URL: https://www.css.cornell.edu/extension/soil-health/front-matter.pdf.

[24] A. P. Edwards, J. M. Bremner, Dispersion of Soil Particles by Sonic Vibration1, Journal of Soil Science 18 (1967) 47–63. doi:10.1111/j.1365-2389.1967.tb01487.x.

[25] J. Schomakers, A. Mentler, T. Steurer, A. Klik, H. Mayer, Characterization of soil aggregate stability using low intensity ultra-

sonic vibrations, International Agrophysics 25 (2011) 165–172.

[26] A. Mentler, H. Mayer, W. E. H. Blum, J. Schomakers, N. Degischer, Measurement of soil aggregate stability using low intensity ultrasonic vibration, Spanish Journal of Soil Science 1 (2014) 109. doi:10.3232/SJSS.2011.V1.N1.01.

[27] J. M. Davison, D. D. Evans, Turbidimeter Technique for Measuring the Stability of Soil Aggregates in a Water-Glycerol Mixture, Soil Science Society of America Journal 24 (1960) 75–79. doi:10.2136/sssaj1960.03615995002400020003x.

[28] Y. Zhu, A. Marchuk, J. McLean Bennett, Rapid Method for Assessment of Soil Structural Stability by Turbidimeter, Soil Science Society of America Journal 80 (2016) 1629–1637. doi:10.2136/sssaj2016.07.0222.

[29] Y. Le Bissonnais, Aggregate stability and assessment of soil crustability and erodibility: I. Theory and methodology, European Journal of Soil Science 47 (1996) 425–437. doi:10.1111/j.1365-2389.1996.tb01843.x.

[30] International Organization for Standardization, ISO 10930, 2012. URL: https://www.iso.org/standard/46433.html.

[31] M. Fajardo, Alex. B. McBratney, D. J. Field, B. Minasny, Soil slaking assessment using image recognition, Soil and Tillage Research 163 (2016) 119–129. doi:10.1016/j.still.2016.05.018.

[32] R Core Team, R: A Language and Environment for Statistical Computing, Vienna, Austria, 2022. URL: https://www.R-project.org/.

[33] M. Fajardo, A. McBratney, Moulder: A soil aggregate stability smart-phone app [Mobile application software]., 2023. URL: https://play.google.com/store/apps/details?id=slaker.sydn

[34] K. D. Flynn, D. K. Bagnall, C. L. Morgan, Evaluation of SLAKES, a smartphone application for quantifying aggregate stability, in high-clay soils, Soil Science Society of America Journal 84 (2020) 345–353. doi:10.1002/saj2.20012.

[35] E. J. Jones, P. Filippi, R. Wittig, M. Fajardo, V. Pino, A. B. McBratney, Mapping soil slaking index and assessing the impact of management in a mixed agricultural landscape, SOIL 7 (2021) 33–46. doi:10.5194/soil-7-33-2021.

[36] D. V. u. Adetsu, M. Lamande, (viaf)71672652 promotor, E. Arthur, (viaf)307217671 promotor, W. u. v. copromotor Cornelis, Evaluating a new method for aggregate stability across soil types and management, Technical Report, 2021., 2021. URL: http://lib.ugent.be/catalog/rug01:003013851.

[37] T. J. Brown, Testing a New Methodology for Measuring Aggregate Stability, Master's thesis, Norwegian University of Life Sciences, Ås, 2021. URL: https://nmbu.brage.unit.no/nmbu-xmlui/handle/11250/2988005.

[38] P. B. Obour, E. Oppong Danso, S. Y. Dorvlo, E. Arthur, Soil aggregate stability quantified by different methods is unaffected by rice straw biochar in the long term, Soil Science Society of America Journal 87 (2023) 1018–1028. doi:10.1002/saj2.20556.

[39] E. L. Rieke, D. K. Bagnall, C. L. S. Morgan, K. D. Flynn, J. A. Howe, K. L. H. Greub, G. Mac Bean, S. B. Cappellazzi, M. Cope, D. Liptzin, C. E. Norris, P. W. Tracy, E. Aberle, A. Ashworth, O. Bañuelos Tavarez, A. I. Bary, R. L. Baumhardt, A. Borbón Gracia, D. C. Brainard, J. R. Brennan, D. Briones Reyes, D. Bruhjell, C. N. Carlyle, J. J. W. Crawford, C. F. Creech, S. W. Culman, B. Deen, C. J. Dell, J. D. Derner, T. F. Ducey, S. W. Duiker, M. F. Dyck, B. H. Ellert, M. H. Entz, A. Espinosa Solorio, S. J. Fonte, S. Fonteyne, A.-M. Fortuna, J. L. Foster, L. M. Fultz, A. V. Gamble, C. M. Geddes, D. Griffin-LaHue, J. H. Grove, S. K. Hamilton, X. Hao, Z. D. Hayden, N. Honsdorf, J. A. Ippolito, G. A. Johnson, M. A. Kautz, N. R. Kitchen, S. Kumar, K. S. M. Kurtz, F. J. Larney, K. L. Lewis, M. Liebman, A. Lopez Ramirez, S. Machado, B. Maharjan, M. A. Martinez Gamiño, W. E. May, M. P. McClaran, M. D. McDaniel, N. Millar, J. P. Mitchell, A. D. Moore, P. A. Moore, M. Mora Gutiérrez, K. A. Nelson, E. C. Omondi, S. L. Osborne, L. Osorio Alcalá, P. Owens, E. M. Pena-Yewtukhiw, H. J. Poffenbarger, B. Ponce Lira, J. R. Reeve, T. M. Reinbott, M. S. Reiter, E. L. Ritchey, K. L. Roozeboom, Y. Rui, A. Sadeghpour, U. M. Sainju, G. R. Sanford, W. F. Schillinger, R. R. Schindelbeck, M. E. Schipanski, A. J. Schlegel, K. M. Scow, L. A. Sherrod, A. L. Shober, S. S. Sidhu, E. Solís Moya, M. St. Luce, J. S. Strock, A. E. Suyker, V. R. Sykes, H. Tao, A. Trujillo Campos, L. L. Van Eerd, H. M. van Es, N. Verhulst, T. J. Vyn, Y. Wang, D. B. Watts, D. L. Wright, T. Zhang, C. W. Honeycutt, Evaluation of aggregate stability methods for soil health, Geoderma 428 (2022) 116156. doi:10.1016/j.geoderma.2022.116156.

[40] M. Madaras, R. Krejčí, M. Mayerová, Assessing soil aggregate stability by measuring light transmission decrease during aggregate disintegration, Soil and Water Research 19 (2024) 25–31. doi:10.17221/78/2023-SWR.

[41] M. Harman, Open Camera, 2024. URL: https://opencamera.org.uk/.

[42] J. Schindelin, I. Arganda-Carreras, E. Frise, V. Kaynig, M. Longair, T. Pietzsch, S. Preibisch, C. Rueden, S. Saalfeld, B. Schmid, J.-Y. Tinevez, D. J. White, V. Hartenstein, K. Eliceiri, P. Tomancak, A. Cardona, Fiji: An open-source platform for biological-image analysis, Nature Methods 9 (2012) 676–682. doi:10.1038/nmeth.2019.

[43] D. Arrouays, C. Jolivet, L. Boulonne, G. Bodineau, N. Saby, E. Grolleau, A new projection in France: A multi-institutional soil quality monitoring network, Comptes Rendus de l'Académie d'Agriculture de France (France) (2002).

[44] M. Peluchon, D. Michot, B. Lemercier, S. Busnot, T. Morvan, M. Fajardo, S. Salvador-Blanes, M. Lacoste, F. Darboux, N. Saby, Evaluation of SLAKES, a smartphone application for quantifying aggregate stability, in soils with contrasting managements (2021) EGU21–14858. doi:10.5194/egusphere-egu21-14858.

[45] J. Cooke, R. Girault, S. Busnot, T. Morvan, S. Menasseri-Aubry, Characterising the Effect of Raw and Post-Treated Digestates on Soil Aggregate Stability, Waste and Biomass Valorization 14 (2023) 2977–2995. doi:10.1007/s12649-023-02045-3.

[46] T. Dorji, D. J. Field, I. O. A. Odeh, Soil aggregate stability and aggregate-associated organic carbon under different land use or land cover types, Soil Use and Management 36 (2020) 308–319. doi:10.1111/sum.12549.

[47] Mario Fajardo, Mobile Apps in Soil Science, 2017. URL: https://www.youtube.com/watch?v=Khd9OKziJyM.

[48] C. V. Bresson, L. M., Soil Crusting, in: Methods for Assessment of Soil Degradation, CRC Press, 1997.

18
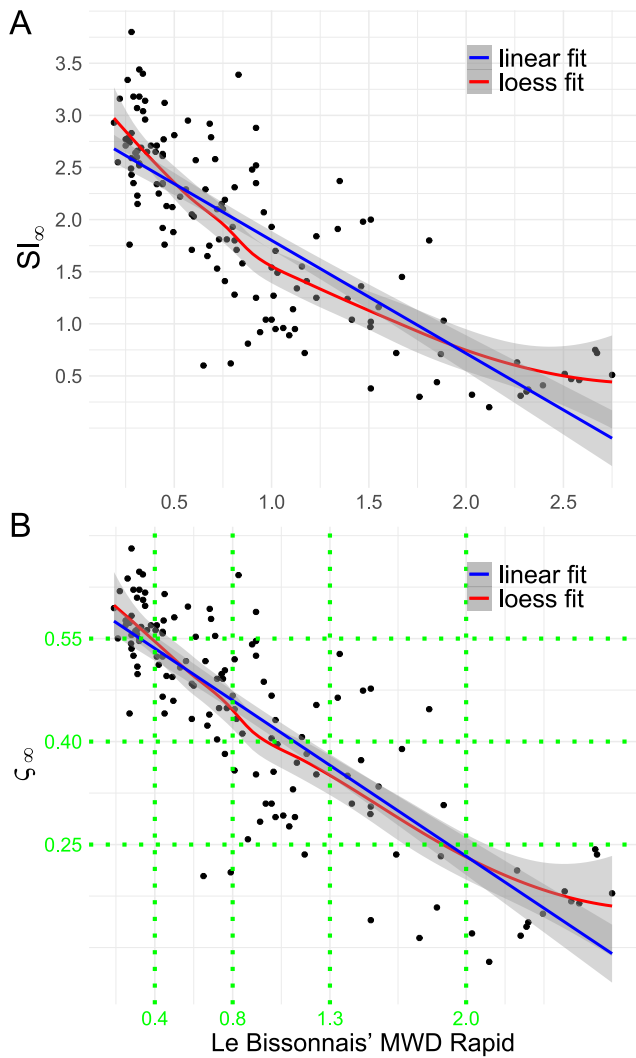
Figure 4: Comparison of ASTAVIT SI_∞ and ς_∞ indices with Le Bissonnais rapid wetting MWD. A: plot of the ASTAVIT SI_∞ index against Le Bissonnais rapid wetting MWD (mm) for the RMQS points having undergone both measures. The LOESS fit is a guide for the eye and the linear fit yields $R^2 = 0.6406$. B: same graph but using the ASTAVIT ς_∞ index. The linear fit yields $R^2 = 0.6857$. The green vertical lines represent the limits for the stability categories from Le Bissonnais, and the horizontal lines are the suggested equivalent limits for ASTAVIT's ς_∞ index.
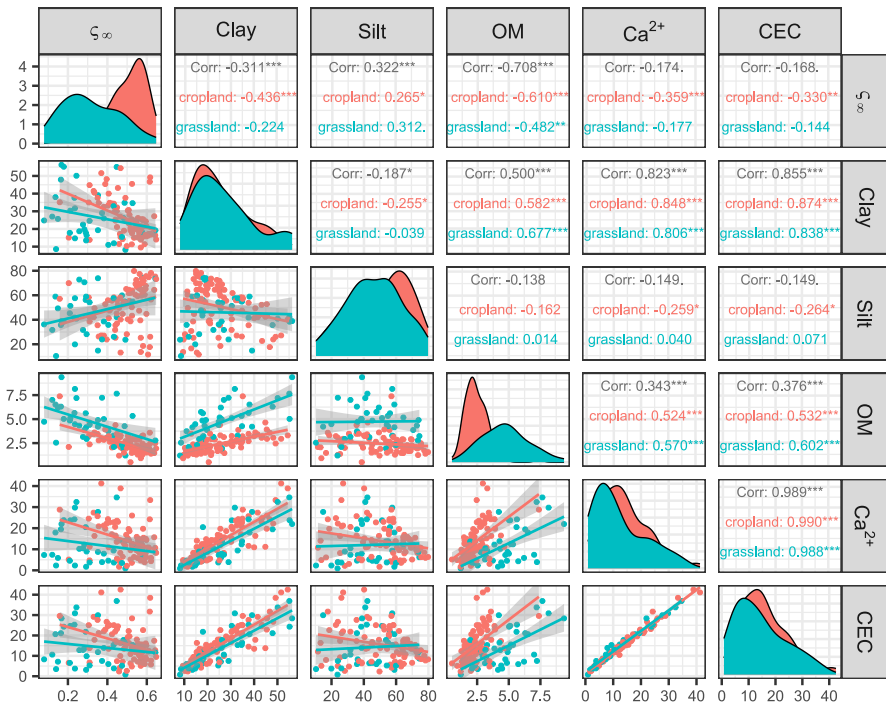
Figure 5: Histograms, point plots and Pearson correlation coefficients between the ASTAVIT ς_∞ index and other soil variables derived from RMQS samples of cropland and grassland. Each point corresponds to one measurement of ASTAVIT (most of times 60 aggregates, and a few times 96 aggregates) on a single RMQS soil sample. A positive correlation between ς_∞ and another parameter indicates a destabilizing effect, while a negative correlation indicates a stabilizing effect of that parameter. Only grassland and cropland sites are considered in this analysis. The binary "soil usage" variable is not present as such, but the samples are separated according to their soil usage and partial correlation coefficients are presented: croplands in orange, and grassland in green.
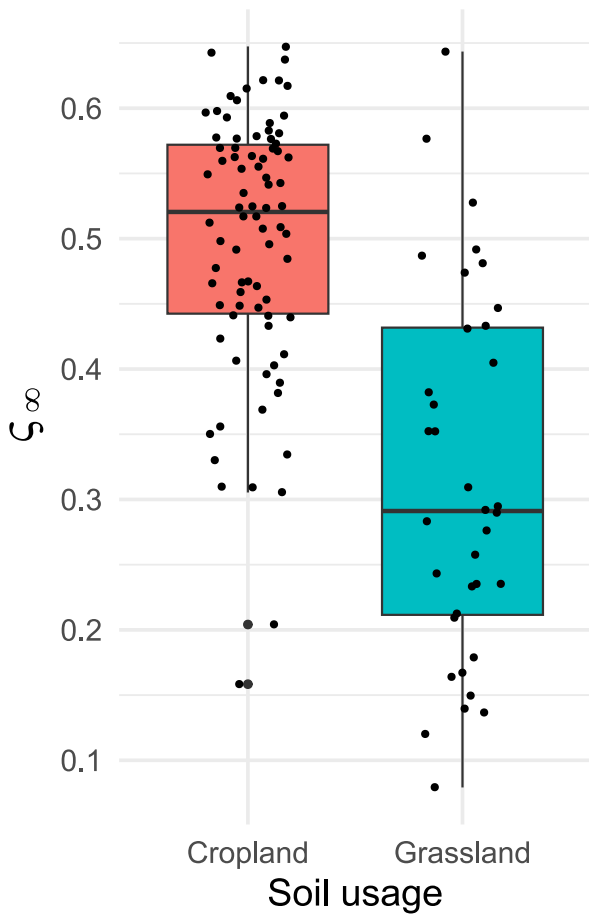
Figure 6: Comparison of the ς_∞ values for cropland and grassland from the selected RMQS samples. Each point corresponds to one measurement of ASTAVIT (most of times 60 aggregates, and a few times 96 aggregates) on a single RMQS soil sample.
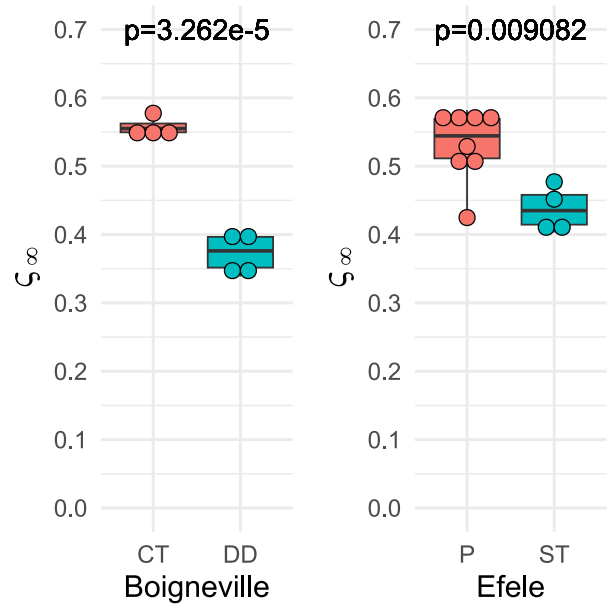

Figure 7: Boxplots of the ASTAVIT ς_∞ index for the Boigneville (CT: conventional tillage; DD: direct-drilled) and EFELE soils (P: plowing; ST: simplified tillage). The individual data points are represented by circles. p-values for the Student's t-test are shown in each case.